OFFPRINT

Dynamic properties of the one-dimensional Bose-Hubbard model

S. EJIMA, H. FEHSKE and F. GEBHARD

TARGET YOUR RESEARCH WITH EPL

Sign up to receive the free EPL table of contents alert.

www.epljournal.org/alerts

Dynamic properties of the one-dimensional Bose-Hubbard model

S. Ejima[1], H. Fehske[1] and F. Gebhard[2]

[1] *Institut für Physik, Ernst-Moritz-Arndt-Universität Greifswald - D-17489 Greifswald, Germany, EU*
[2] *Department of Physics, Philipps-Universität Marburg - D-35032 Marburg, Germany, EU*

Abstract – We use the density-matrix renormalization group method to investigate ground-state and dynamic properties of the one-dimensional Bose-Hubbard model, the effective model of ultracold bosonic atoms in an optical lattice. For fixed maximum site occupancy $n_b = 5$, we calculate the phase boundaries between the Mott insulator and the "superfluid" phase for the lowest two Mott lobes. We extract the Tomonaga-Luttinger parameter from the density-density correlation function and determine accurately the critical interaction strength for the Mott transition. For both phases, we study the momentum distribution function in the homogeneous system, and the particle distribution and quasi-momentum distribution functions in a parabolic trap. With our zero-temperature method we determine the photoemission spectra in the Mott insulator and in the "superfluid" phase of the one-dimensional Bose-Hubbard model. In the insulator, the Mott gap separates the quasi-particle and quasi-hole dispersions. In the "superfluid" phase the spectral weight is concentrated around zero momentum.

Introduction. – At very low temperatures, bosonic atoms which are loaded into an optical lattice become superfluid for a shallow optical potential and Mott insulators for a deep optical potential. The transition between both phases has been observed experimentally [1]; for a recent review, see [2]. The Bose-Hubbard model provides a reasonable description of the experimental situation, and its ground-state phase diagram in two and three dimensions has been determined fairly accurately by perturbation theory [3–5] and quantum Monte Carlo (QMC) calculations [6–8].

Bosons on a chain are also accessible experimentally [9] so that it is interesting to study the one-dimensional Bose-Hubbard model. The physics in one dimension is rather peculiar. For example, the state with the lowest kinetic energy is not macroscopically occupied in the "superfluid" [10] but it is characterised by an algebraic divergence of the momentum distribution; for a review, see [11]. Moreover, the Mott gap is exponentially small in the Mott insulator close to the phase transition. Therefore, it is very difficult to determine the critical interaction strength numerically. This problem also impairs the applicability of strong-coupling perturbation theory.

In one dimension and at zero temperature, the density-matrix renormalisation group (DMRG) method [12–14] permits the calculation of ground-state properties with an excellent accuracy for large systems so that the extrapolation to the thermodynamic limit can be performed reliably. In this work, we use the density-density correlation function to calculate the Tomonaga-Luttinger parameter from which we determine the Mott transition accurately. Moreover, we obtain the momentum distribution and the particle distribution for bosons on a homogeneous chain and in the presence of a harmonic trap. Using the dynamical DMRG [15], we calculate the single-particle spectral function at zero temperature in the "superfluid" and the Mott insulating phases.

Bose-Hubbard model. – The Hamilton operator for the Bose-Hubbard model on a chain with an even number of sites L in a harmonic potential is defined by

$$\hat{\mathcal{H}} = -t \sum_j \left(\hat{b}_j^\dagger \hat{b}_{j+1} + \hat{b}_{j+1}^\dagger \hat{b}_j \right) + \frac{U}{2} \sum_j \hat{n}_j (\hat{n}_j - 1)$$
$$+ V_c \sum_j (j - r_c)^2 \, \hat{n}_j, \tag{1}$$

where $\hat{b}_j^\dagger$ and $\hat{b}_j$ are the creation and annihilation operators for bosons on site j, $\hat{n}_j = \hat{b}_j^\dagger \hat{b}_j$ is the boson number operator on site j, t is the tunnel amplitude between

neighbouring lattice sites, $U > 0$ denotes the strength of the on-site Coulomb repulsion, V_c parameterises the curvature of the quadratic confining potential, and $r_c = (L+1)/2$ denotes the central position of the chain. In the following, we set $U = 1$ as our energy unit, unless stated otherwise.

Constrained Bose-Hubbard model. In general, the Bose-Hubbard model cannot be solved analytically. In the low-density limit, the model reduces to the Bose gas with δ-potential interaction which was solved by Lieb and Liniger [16]. The fact that three or more bosons may occupy the same site forms the major obstacle on the way to an exact solution. Since multiple occupancies also pose technical problems in numerical approaches, the Bose-Hubbard model is usually approximated by the constraint that there is a maximal number of bosons per site, $0 \leqslant n_b \leqslant \mathcal{N} - 1$. This constrained Bose-Hubbard model has $\mathcal{N}$ degrees of freedom per site so that it can be written in terms of spin variables with $S = (\mathcal{N} - 1)/2$. The case $\mathcal{N} = 2$ is trivial because the hard-core Bose-Hubbard model has no interaction term. It reduces to a model for free spinless fermions whose properties are known exactly [17]. The Bose-Hubbard model is recovered in the limit $\mathcal{N} \to \infty$. In general, however, the $SU(\mathcal{N})$-Bethe Ansatz equations do not solve the constrained Bose-Hubbard model [18,19].

In our work, we study the restricted Bose-Hubbard model with $\mathcal{N} = 6$, *i.e.*, $n_b \leqslant 5$. Our results are representative for the original Bose-Hubbard model (1) because multiple lattice occupancies are strongly suppressed in the parameter regions of interest to us, $U/t > 2$ and fillings $\rho = N/L < n_b$.

Numerical algorithm. We adopt the DMRG method [12] as our numerical tool for the calculation of ground-state properties for constrained Bose systems [13,14]. For the spectral properties, we employ the dynamical DMRG (DDMRG) [15].

The considered lattices are large enough to permit reliable extrapolations to the thermodynamic limit for the physical quantities of interest to us. We keep up to $m = 2000$ density-matrix eigenstates, so that the discarded weight is always smaller than 1×10^{-10}.

We checked our algorithm for $n_b = 1$ against the exact result [17]. The exact ground-state energy in the thermodynamical limit and the extrapolated ground-state energy from DMRG agree to four-digit accuracy.

Ground-state phase diagram. At integer filling $\rho = N/L$, the Bose-Hubbard model in one dimension describes a Mott transition between the "superfluid" phase, characterised by a divergence of the momentum distribution at momentum $k = 0$ [10], and a Mott insulating phase, characterised by a finite gap for single-particle excitations. The latter is defined by the energy difference between the chemical potentials for half band filling and one particle
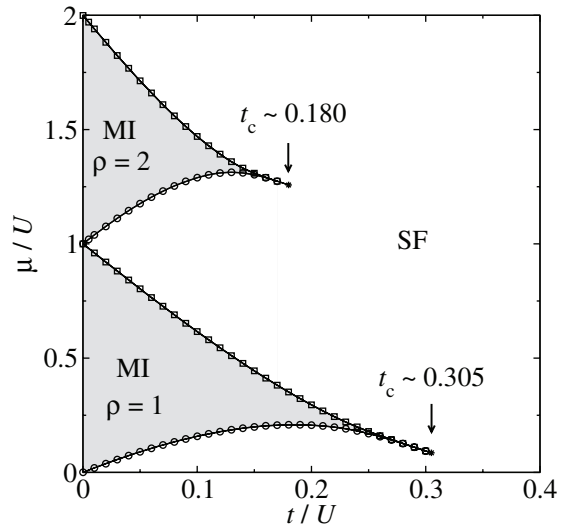

Fig. 1: Phase diagram of the one-dimensional constrained Bose-Hubbard model ($n_b \leqslant 5$) from DMRG with "superfluid" (SF) and Mott insulating (MI) regions. The symbols confine the regions with a finite Mott gap, $\Delta > 0$, extrapolated from $\Delta(L)$ for $L \leqslant 128$. The position of the Mott tips has been obtained from the Tomonaga-Luttinger parameter.

less than half filling,

$$\Delta(L) = \mu^+(L) - \mu^-(L),$$
$$\mu^+(L) = E_0(L, N+1) - E_0(L, N), \qquad (2)$$
$$\mu^-(L) = E_0(L, N) - E_0(L, N-1),$$

where $E_0(L, N)$ is the ground-state energy for L sites and N particles. In the thermodynamical limit, $N, L \to \infty$ and $\rho = N/L$ integer, the gap is finite for the Mott insulator, $\Delta = \lim_{N,L\to\infty} \Delta(L) > 0$, so that the system becomes incompressible when we go from the "superfluid" phase to the Mott insulating phase.

The Mott transition lines in the μ-U ground-state phase diagram have been previously determined by various analytical and numerical methods, *e.g.*, strong-coupling expansions [20,21], variational cluster approach [22], QMC [23,24], and DMRG [13,14]. In fig. 1 we show the phase diagram for the first Mott lobe ($\rho = 1$) and the second Mott lobe ($\rho = 2$) as obtained from our DMRG calculations with system sizes up to $L = 128$.

The overall shape of the Mott lobes agrees with previous results. Here, we provide accurate data for the second Mott lobe, and the values for the critical interaction strength for the first two Mott lobes which we obtain from the Tomonaga-Luttinger parameter. At the tip of each Mott lobe, the model is in the universality class of the XY spin model so that there is a Kosterlitz-Thouless phase transition with the Tomonaga-Luttinger parameter $K_b = 1/2$, and the gap is exponentially small in the vicinity of $(t/U)_c$. In contrast, $SU(\mathcal{N})$-Bethe Ansatz equations

predict a discontinuity of the gap at the critical interaction for $\mathcal{N} \geqslant 3$ [18,19].

Ground-state properties. –

Tomonaga-Luttinger parameter and critical interactions for the Mott transition. The low-energy excitations of interacting bosons in the superfluid phase are gapless linear excitations ("phonons"). As in the case of fermionic systems in one dimension [25,26], the Tomonaga-Luttinger parameter K_b determines the asymptotic behaviour of the correlation functions in the "superfluid" phase, and various correlations functions have been used to extract K_b [27–30]. Here, we employ the density-density correlation function which is defined by the ground-state expectation value

$$C(r) = \frac{1}{L} \sum_{\ell=1}^{L} \langle \hat{n}_{\ell+r} \hat{n}_\ell \rangle - \langle \hat{n}_{\ell+r} \rangle \langle \hat{n}_\ell \rangle. \tag{3}$$

Asymptotically, it behaves like

$$C(r \to \infty) \sim -\frac{1}{2K_b} \frac{1}{(\pi r)^2} + \frac{A\rho^2 \cos(2\pi\rho r)}{(\rho r)^{2/K_b}} + \cdots. \tag{4}$$

Thus, we can extract K_b from the derivative of its Fourier transformation,

$$\tilde{C}(q) = \sum_{r=1}^{L} e^{-\mathrm{i}qr} C(r), \quad 0 \leqslant q < 2\pi, \tag{5}$$

as $q = 0$. In the thermodynamic limit one finds

$$\frac{1}{2\pi K_b} = \lim_{q \to 0} \frac{\tilde{C}(q)}{q}. \tag{6}$$

In order to treat finite systems in numerical calculations [26], we translate (6) into

$$\frac{1}{2K_b(L)} = \lim_{L \to \infty} \frac{L}{2} \tilde{C}\left(\frac{2\pi}{L}\right), \tag{7}$$

and extrapolate $K_b(L)$ to the thermodynamical limit.

In refs. [14] and [31] the transition point has been also determined from the Luttinger parameter K_b. However, these authors estimated K_b from the single-particle density matrix

$$\Gamma(r) = \langle \hat{b}_r^\dagger \hat{b}_0 \rangle \sim r^{-K_b/2} \text{ for } r \gg 1. \tag{8}$$

In their work, the extrapolation for the critical point t_c depends on the interval used for the fits to $\Gamma(r)$, see table I in ref. [14]. When we derive the Luttinger parameter from eq. (6) we can avoid this problem.

As shown in fig. 2, $K_b(L)$ can be reliably extrapolated to the thermodynamic limit using polynomial functions in $1/L$. For $\rho = 1$, we clearly have $K_b(t/U = 0.3) > 1/2$. When we extrapolate our data for up to $L = 1024$ lattice sites, we find $K_b(t/U = 0.304) > 1/2$ but $K_b(t/U = 0.306) < 1/2$. Therefore, we locate the transition point at $t_c = 0.305 \pm$
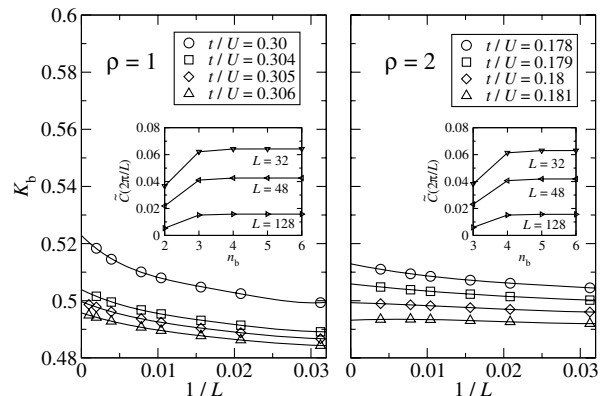

Fig. 2: Finite-size scaling for the Tomonaga-Luttinger parameter K_b in the one-dimensional constrained Bose-Hubbard model ($n_b = 5$) for the first ($\rho = 1$) and second ($\rho = 2$) Mott lobes, using the DMRG with open boundary conditions. The lines are polynomial fits. The insets give the n_b-dependence of $\tilde{C}(2\pi/L)$ for various system sizes at $t/U = 0.305$ (left panel) and $t/U = 0.18$ (right panel).

0.001 for the first Mott lobe. In the same way we find the transition point for the second Mott lobe at $t_c = 0.180 \pm 0.001$ for the restricted Bose-Hubbard model with $n_b \leqslant 5$. Using the same method, we have verified numerically that the values for the critical coupling $(t/U)_c$ are the same for $n_b = 4, 6$ within our extrapolation uncertainty.

Note that $K_b(t < t_c)$ is not defined because we are in the Mott insulating phase. However, $K_b(L)$ is finite and continuous over the Kosterlitz-Thouless transition because the Mott gap is exponentially small near t_c. Nevertheless, our approach remains applicable as has been shown for various fermionic models in refs. [26,32].

Previous groups located the Kosterlitz-Thouless transition for the first Mott lobe at values consistent with ours. In their DMRG work [14], Kühner *et al.* computed the Luttinger parameter using their DMRG algorithm on lattices with up to $L = 1024$ sites. From their fit to $\Gamma(r)$, eq. (8), they found $t_c = 0.297 \pm 0.01$. Based on the same correlation function, Zakrzewski and Delande [31] gave $t_c = 0.2975 \pm 0.005$ for the first and $t_c = 0.175 \pm 0.002$ for the second Mott lobe for $n_b = 6$. The determined t_c-values of such a kind significantly depend on the interval of r, which is not the case within our approach. Läuchli and Kollath [33] determined the critical point from the block entropy, by combining the recently developed quantum information theory with the DMRG. Our result is within their region of the estimated values for t_c (see fig. 2 in ref. [33]). In a combination of an exact diagonalisation study for systems with up to $L = 12$ sites and a renormalisation group approach, Kashurnikov and Svistunov found $t_c = 0.304 \pm 0.002$ [34], and their QMC calculations together with Kravasin gave $t_c = 0.300 \pm 0.005$ [24]. Another QMC calculation in combination with a renormalisation-group flow analysis of the finite-temperature data gave $t_c = 0.305(4)$ [35], in
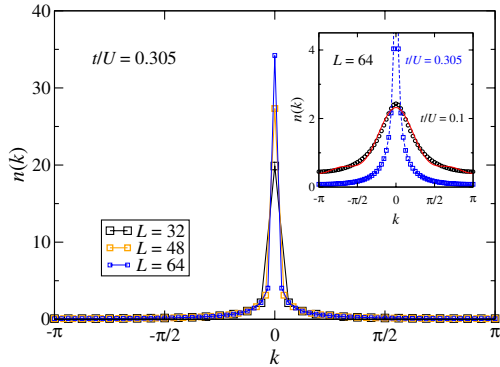
Fig. 3: (Colour on-line) Finite-size dependence of the momentum distribution function $n(k)$ for $t = 0.1$ (Mott insulator) and $t = 0.305$ ("superfluid") in the one-dimensional Bose-Hubbard model using the DMRG with periodic boundary conditions. Inset: $n(k)$ for $L = 64$. The solid line in the inset gives the result of strong-coupling theory to third order, eq. (10) [5,37].
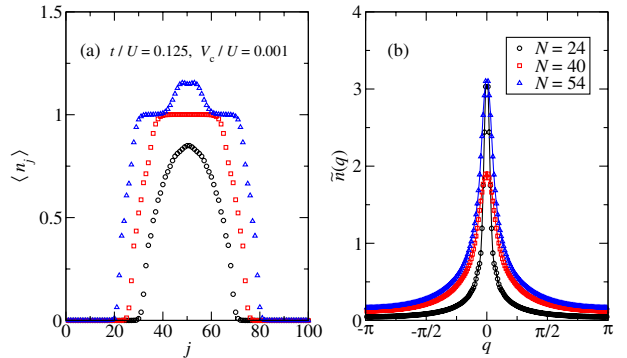

Fig. 4: (Colour on-line) Occupation probabilities in the one-dimensional constrained Bose-Hubbard model ($n_b \leqslant 5$) in a parabolic trap potential of strength $V_c/U = 0.001$. We show the results for $N = 24, 40, 54$ and $L = 100$ ($\rho = 0.24, 0.40, 0.54$) for $t/U = 0.125$ for (a) the local densities $\langle \hat{b}_j^\dagger \hat{b}_j \rangle$ and (b) the pseudo-momentum distribution $\widetilde{n}(q)$.

perfect agreement with the result of our zero-temperature study.

Momentum distribution function. — Using the DMRG, the momentum distribution function $n(k)$ can be calculated by taking the Fourier transformation of the single-particle density matrix

$$n(k) = \frac{1}{L} \sum_{j,\ell=1}^{L} e^{ik(j-\ell)} \langle \hat{b}_j^\dagger \hat{b}_\ell \rangle, \qquad (9)$$

where $k = 2\pi m/L$ for $m = -L/2 - 1, \ldots, L/2$ holds for periodic boundary conditions [36]. Note that the momentum distribution function fulfils the sum rule $\sum_k n(k) = N$. In all cases of fig. 3 the numerical deviation $\xi = |N - \sum_k n(k)|$ is always small, $\xi < 1.0 \times 10^{-3}$.

The difference between the superfluid phase and the Mott insulator is most markedly seen in the momentum distribution $n(k)$ at momentum $k = 0$: in the insulating phase, $n(k = 0)$ remains finite whereas it diverges as a function of system size in the superfluid phase, as shown in fig. 3. At $t/U = 0.1$, $n(k = 0)$ is almost independent of system size, and the momentum distribution $n(k)$ is a smooth function of momentum k. Strong-coupling perturbation theory to third order [5,37] predicts ($x = t/U$)

$$n^{[3]}(k) = 1 + 2C_1 \cos(k) + 2C_2 \cos(2k) + 2C_3 \cos(3k),$$
$$C_1 = 4x - 8x^3, \quad C_2 = 18x^2, \quad C_3 = 88x^3. \qquad (10)$$

Our numerical results for $t/U = 0.1$ favourably compare with this expression, see the inset of fig. 3.

At $t/U = 0.305$, above the critical point, $n(k = 0)$ increases rapidly with system size. In one spatial dimension there is no true superfluid with a macroscopic value for $n(k = 0)$ in the thermodynamic limit [10]. Instead, we have from (8) $n(|k| \to 0) \sim |k|^{-\nu}$, $\nu = 1 - K_b/2 < 1$.

Local densities for the Bose-Hubbard model in a trap. — In the presence of the confining potential V_c in the model (1), the density profile over the trap is no longer homogeneous, see, *e.g.*, ref. [38]. For an open system, we define the quasi-momentum distribution $\widetilde{n}(q) = \langle \hat{b}^\dagger(q)\hat{b}(q) \rangle$ using the quasi-momentum states of particles in a box,

$$\hat{b}(q) = \sqrt{\frac{2}{L+1}} \sum_\ell \sin(q\ell)\hat{b}_\ell \qquad (11)$$

with $q = \pi n_q/(L+1)$ for integers $1 \leqslant n_q \leqslant L$.

As demonstrated by Batrouni *et al.* [38] and Kollath *et al.* [36], the potential confines the particles in the middle of the trap. For small fillings, the local occupancies display a bell-shaped distribution, where the maximum does not reach the Mott plateau value, $\langle \hat{b}_j^\dagger \hat{b}_j \rangle (\rho = 0.24) < 1$. The quasi-momentum distribution $\widetilde{n}(q)$ for this "superfluid in a trap" shows a prominent peak at $k = 0$. For a larger filling, $\rho = 0.40$, there exists a Mott plateau, $\langle \hat{b}_j^\dagger \hat{b}_j \rangle (\rho = 0.40) = 1$ for $40 < j < 60$. Recall that, for $t/U = 0.125$, the homogeneous system at filling $\rho = 1$ is a Mott insulator. Correspondingly, the peak in the pseudo-momentum distribution at $k = 0$ is smaller for $\rho = 0.40$ than for $\rho = 0.24$, see fig. 4(b). Finally, at filling $\rho = 0.54$, the confining potential and the bosons' tendency to cluster overcome the repulsive potential in the middle of the trap so that local occupancies larger than unity are seen inside the trap. Correspondingly, the peak intensity of the pseudo-momentum distribution at $\rho = 0.54$ exceeds its value for $\rho = 0.40$.

Photoemission spectra. – Single-particle excitations associated with the injection or emission of a boson with wave vector q and frequency ω, $A^+(q, \omega)$ or $A^-(q, \omega)$, are described by the spectral functions

$$A^\pm(q, \omega) = \sum_n |\langle \psi_n^\pm | \hat{b}^\pm(q) | \psi_0 \rangle|^2 \delta(\omega \mp \omega^\pm), \qquad (12)$$
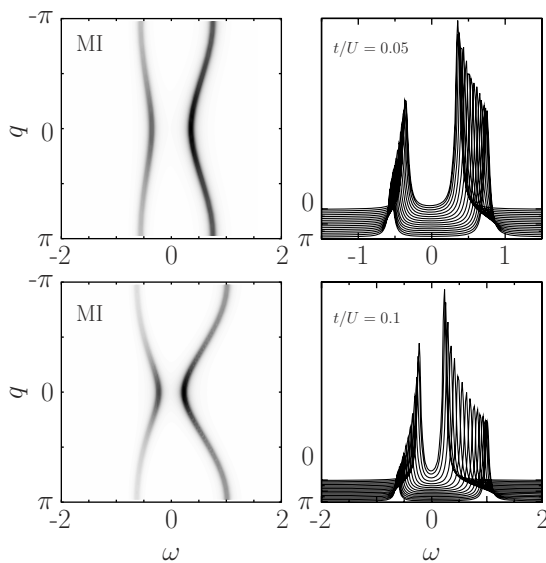
Fig. 5: Intensity (left panels) and line-shape (right panels) of the single-boson spectral functions $A(q,\omega)$ in the Mott insulating (MI) phase for $t/U = 0.05$ (upper panels) and $t/U = 0.1$ (lower panels) with system size $L = 64$ at filling $\rho = 1$ using the DDMRG technique with open boundary conditions.

where $\hat{b}^+(q) = \hat{b}^\dagger(q)$ and $\hat{b}^-(q) = \hat{b}(q)$ create/annihilate particles with pseudo-momentum q. Moreover, $|\psi_0\rangle$ is the ground state of a L-site system in the N-particle sector while $|\psi_n^\pm\rangle$ denote the n-th excited states in the $(N\pm1)$-particle sectors with excitation energies $\omega_n^\pm = E_n^\pm - E_0$.

So far, very few data are available for the (inverse) photoemission spectra in the one-dimensional (constrained) Bose-Hubbard model. Analytical results include the variational cluster perturbation theory [22], the random phase approximation [39], and strong-coupling theory [40]. Pippan *et al.* [41] combined QMC at low but finite temperatures with the maximum-entropy method to extract the spectral functions.

In the following we present the (inverse)-photoemission spectra at zero temperature using the numerically exact dynamical DMRG method [15,42]. We keep $m = 500$ states to obtain the ground state in the first five DMRG sweeps and take $m = 200$ states for the calculation of the various spectra from (12) by DDMRG. For a bosonic system the following sum-rules hold:

$$\int_{-\infty}^{\infty} \mathrm{d}\omega \left(A^+(k,\omega) - A^-(k,\omega) \right) = 1, \qquad (13)$$

$$\int_{-\infty}^{0} \mathrm{d}\omega \left(A^+(k,\omega) + A^-(k,\omega) \right) = n(k). \qquad (14)$$

In our DDMRG calculations, both sum-rules are fulfilled with high precision.

In fig. 5 we show the results for the Mott insulator with $\rho = 1$. The spectra $A(q,\omega) = A^+(q,\omega) + A^-(q,\omega)$ for fixed q consist of two Lorentzians of width $\eta = 0.04$, the size of the broadening introduced in the DDMRG procedure. The
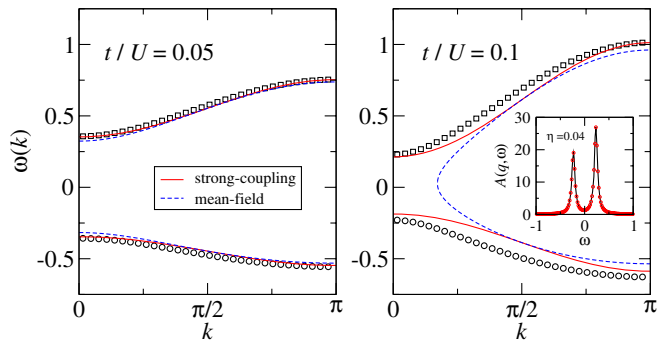

Fig. 6: (Colour on-line) Quasi-particle dispersions $\omega(k)$ in the Mott insulating phase at filling $\rho = 1$ for $t/U = 0.05$ and $t/U = 0.1$ from Lorentz fits to the spectral functions $A(q,\omega)$. For comparison, we also show the strong-coupling dispersions for the propagation of a hole and a double occupancy, $\omega_{\mathrm{h,p}}(k)$, and the mean-field result of ref. [40]. Inset: $A(q,\omega)$ for $t/U = 0.1$ at $q = \pi/33$ with $L = 32$ (line) and $q = 2\pi/65$ with $L = 64$ (circles) demonstrating the negligible system size dependence.
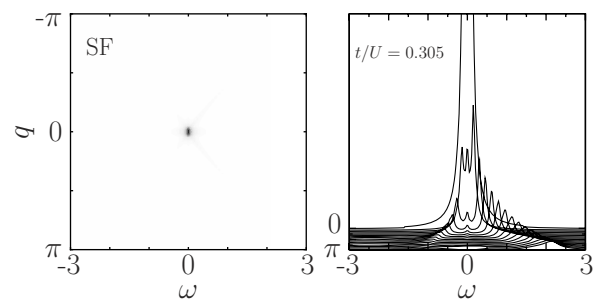

Fig. 7: Intensity (left panel) and line-shape (right panel) of the single-boson spectral functions $A(q,\omega)$ for $t_c = 0.305$ ("superfluid" phase) with system size $L = 64$ at filling $\rho = 1$ using the DDMRG technique with open boundary conditions for a broadening $\eta = 0.04$.

quality of the fits suggests that the quasi-particle life-time is very large in the Mott insulator.

In fig. 6 we show the quasi-particle dispersions for $t/U = 0.05$ and $t/U = 0.1$ which we extracted from the fits of the spectral functions to two Lorentz peaks at $\omega = \omega^\pm(k)$. For comparison, we include the mean-field result [40] and the strong-coupling result. For large interactions, each site is singly occupied in the ground state. A hole excitation can propagate freely so that the dispersion relation is given by $\omega_{\mathrm{h}}(k) = -\mu + 2t\cos(k)$. Likewise, a doubly occupied site can also move freely through the system. Since either of the two bosons of the doubly occupied site can tunnel to its neighbouring sites, the dispersion relation is given by $\omega_{\mathrm{p}}(k) = U - \mu - 4t\cos(k)$. These expressions for the quasi-particle dispersions are exact to leading and first order in strong-coupling perturbation theory.

In fig. 7 we show the spectral functions in the "superfluid" phase for $\rho = 1$ close to the Mott transition, $t = 0.305$. The elementary excitations concentrate around ($k = 0, \omega = 0$). This confirms the formation of a "condensate",

as also seen in the momentum distribution, see fig. 3. Moreover, it shows that the low-energy excitations near $k = 0$ indeed dominate the spectral functions. We used this concept for the analysis of the ground-state correlation functions, see eq. (4). Note that deep inside of the Mott phase the system size dependence of the spectral functions is insignificant, see inset of fig. 6.

Conclusions. – In this work we have investigated the one-dimensional constrained Bose-Hubbard model ($n_b \leqslant 5$) at zero temperature. Using the density-matrix renormalisation group method we have obtained the Tomonaga-Luttinger parameter K_b from the density-density correlation function and determined the critical couplings $(t/U)_c = 0.305(1)$ for density $\rho = N/L = 1$ and $(t/U)_c = 0.180(1)$ for density $\rho = 2$ which separate the "superfluid" and Mott insulating phases.

In the "superfluid" phase, the momentum distribution diverges for small momenta, $n(|k| \to 0) \sim |k|^{-\nu} \sim L^{\nu}$ ($\nu = 1 - K_b/2$), and the spectral function is finite only for small frequencies and momenta. In the presence of a confining potential, we recover the Mott plateau in the particle density for filling $\rho = 0.40$ and the wedding-cake structure for filling $\rho = 0.54$.

In the Mott insulator, the momentum distribution is a continuous function. The spectral function is well described in terms of free quasi-hole and quasi-particle excitations which have a very long life-time for strong correlations. Their dispersion relation can be obtained from strong-coupling perturbation theory. A calculation of the quasi-particle bands beyond first order remains to be done.

$$* * *$$

REFERENCES

[1] Greiner M., Mandel O., Esslinger T., Hänsch T. W. and Bloch I., *Nature*, **415** (2002) 39.
[2] Bloch I., Dalibard J. and Zwerger W., *Rev. Mod. Phys.*, **80** (2008) 885.
[3] Fisher M. P. A. *et al.*, *Phys. Rev. B*, **40** (1989) 546.
[4] Teichmann N. *et al.*, *Phys. Rev. B*, **79** (2009) 224515.
[5] Freericks J. K. *et al.*, *Phys. Rev. A*, **79** (2009) 053631.
[6] Capogrosso-Sansone B., Prokof'ev N. V. and Svistunov B. V., *Phys. Rev. B*, **75** (2007) 134302.
[7] Kato Y., Zhou Q., Kawashima N. and Trivedi N., *Nat. Phys.*, **4** (2008) 617.
[8] Capogrosso-Sansone B. *et al.*, *Phys. Rev. A*, **77** (2008) 015602.
[9] Stöferle T. *et al.*, *Phys. Rev. Lett.*, **92** (2004) 130403.
[10] Mora C. and Castin Y., *Phys. Rev. A*, **67** (2003) 053615.

[11] Giamarchi T., *Quantum Physics in One Dimension* (Oxford University Press, Oxford) 2004.
[12] White S. R., *Phys. Rev. Lett.*, **69** (1992) 2863; *Phys. Rev. B*, **48** (1993) 10345.
[13] Kühner T. D. and Monien H., *Phys. Rev. B*, **58** (1998) R14741.
[14] Kühner T. D., White S. R. and Monien H., *Phys. Rev. B*, **61** (2000) 12474.
[15] Jeckelmann E., *Phys. Rev. B*, **66** (2002) 045114.
[16] Lieb E. H. and Liniger W., *Phys. Rev.*, **130** (1963) 1605; Lieb E. H., *Phys. Rev.*, **130** (1963) 1616.
[17] Lieb E., Schultz T. and Mattis D., *Ann. Phys. (N.Y.)*, **16** (1961) 407.
[18] Frahm H. and Schadschneider A., in *The Hubbard Model*, edited by Baeriswyl D. *et al.* (Plenum Press, New York) 1995, p. 21.
[19] Frahm H. and Schadschneider A., *J. Phys. A: Math. Gen.*, **26** (1993) 1463.
[20] Freericks J. K. and Monien H., *Phys. Rev. B*, **53** (1996) 2691.
[21] Elster N. and Monien H., *Phys. Rev. B*, **59** (1999) 12184.
[22] Koller W. and Dupuis N., *J. Phys.: Condens. Matter*, **18** (2006) 9525.
[23] Batrouni G. G. and Scalettar R. T., *Phys. Rev. B*, **46** (1992) 9051.
[24] Kashurnikov V. A., Krasavin A. V. and Svistunov B. V., *Pis'ma Zh. Eksp. Teor. Fiz.*, **64** (1996) 92 (*JETP Lett.*, **64** (1996) 99).
[25] Sengupta P., Sandvik A. W. and Campbell D. K., *Phys. Rev. B*, **65** (2002) 155113.
[26] Ejima S., Gebhard F. and Nishimoto S., *Europhys. Lett.*, **70** (2005) 492.
[27] Haldane F. D. M., *Phys. Rev. Lett.*, **47** (1981) 1840.
[28] Giamarchi T., *Phys. Rev. B*, **46** (1992) 342.
[29] Moseley C., Fialko O. and Ziegler K., *Ann. Phys. (Berlin)*, **17** (2008) 561.
[30] Shashi A. *et al.*, arXiv:1010.2268.
[31] Zakrzewski J. and Delande D., *AIP Conf. Proc.*, **1076** (2008) 292.
[32] Ejima S. and Nishimoto S., *Phys. Rev. Lett.*, **99** (2007) 216403.
[33] Läuchli A. M. and Kollath C., *J. Stat. Mech.* (2008) P05018.
[34] Kashurnikov V. A. and Svistunov B. V., *Phys. Rev. B*, **53** (1996) 11776.
[35] Rombouts S. M. A., Van Houcke K. and Pollet L., *Phys. Rev. Lett.*, **96** (2006) 180603.
[36] Kollath C. *et al.*, *Phys. Rev. A*, **69** (2004) 031601(R).
[37] Damski B. and Zakrzewski J., *Phys. Rev. A*, **74** (2006) 043609.
[38] Batrouni G. G. *et al.*, *Phys. Rev. Lett.*, **89** (2002) 117203.
[39] Menotti C. and Trivedi N., *Phys. Rev. B*, **77** (2008) 235120.
[40] Van Oosten D., van der Straten P. and Stoof H. T. C., *Phys. Rev. A*, **63** (2001) 053601.
[41] Pippan P., Evertz H. G. and Hohenadler M., *Phys. Rev. A*, **80** (2009) 033612.
[42] Jeckelmann E. and Fehske H., *Riv. Nuovo Cimento*, **30** (2007) 259.